



Biomedical Engineering

---

# GRADUATE RESEARCH DAY SPRING 2020

---

DISCOVER | DEVELOP | DELIVER



***Be Worlds  
Ahead***

# **FIU** | Engineering & Computing

Biomedical Engineering

## *9th Annual* **Graduate Research Day** **Friday March 6<sup>th</sup>, 2020**

**9:00 AM**

**Seminar with Daniela Cadena and  
Robert Hacker (EC 2300)**

**10:30 AM**

**Students Poster Session (Panther Pit)**

**1:00 PM**

**Students Oral Presentation (EC 2300)**

**3:00 PM**

**Seminar with Dr. Mark A. Anastasio (EC 2300)**

**4:00 PM**

**Awards Ceremony (EC 2300)**

**Florida International University Engineering Center**

**10555 W Flagler St. Miami, FL 33174**

# MESSAGE FROM THE CHAIR

*Congratulations, Biomedical Engineering Graduate Students!*

*Today we celebrate your achievements. You serve as the backbone of our Department, and you continue to push us to new heights. We are proud of your hard work and dedication in advancing human knowledge and developing technologies that will transform the future of medicine. Research involves pushing the limits of our collective understanding, which requires inquisitiveness, resiliency, creativity, innovation, and intelligence.*

*The work that you present today demonstrates that you have the necessary attributes to conduct research at the highest level. The Graduate Research Day provides an opportunity to reflect on your accomplishments and showcase your work with pride.*

*As you move forward in your graduate education, continue motivating yourself and others around you to enhance your knowledge, remain inquisitive, and continue to grow in all aspects of learning.*

*Thank you to all who have worked to make this Graduate Research Day a success!*

*Best wishes for continued success,*

A handwritten signature in black ink, appearing to read 'Ranu Jung', with a stylized flourish at the end.

Ranu Jung, PhD  
Chair, Biomedical Engineering

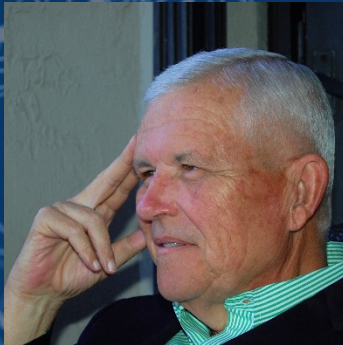


# GUEST SPEAKERS

DANIELA CADENA is a growth designer, with over seven years experience in product development and customer experience. She founded her first company in 2012; as an entrepreneur she discovered her commitment to solving social problems through profit-driven models. This led her in discovering her passion for sustainable business models and practices. Her heart is in her work, where she encourages inventors to problem solve the complex problems our world is facing with sustainable solutions that leverage emerging technologies of the Fourth Industrial Revolution.



**Daniela Cadena**  
Director of Venture  
Ready Programs,  
StartUP FIU



**Robert Hacker**  
Director of StartUP FIU,  
Professor FIU

ROBERT HACKER joined FIU in 2005 and has taught entrepreneurship at ECS since 2010. Prior to FIU he built a billion dollar public company in Asia. He also served as CFO of One Laptop per Child for three years. He has taught a social entrepreneurship course at MIT Sloan School of Management since 2011.

DR. MARK ANASTASIO is the Donald Biggar Willett Professor in Engineering and the Head of the Department of Bioengineering at the University of Illinois at Urbana-Champaign (UIUC). Before joining UIUC in 2019, he was a Professor of Biomedical Engineering at Washington University in St. Louis, where he established one of the nation's first stand-alone PhD programs in imaging science.



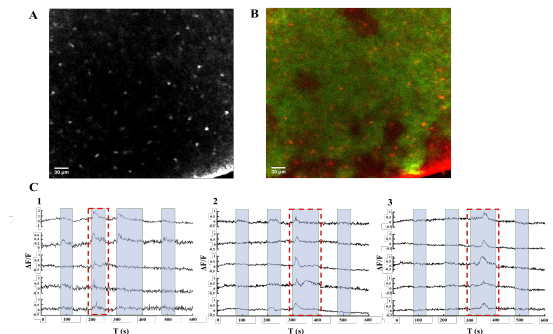
**Dr. Mark A. Anastasio**  
Professor and Head of Bioengineering:  
University of Illinois at Urbana-Champaign

# Channelrhodopsin 2 - Driven $\text{Ca}^{2+}$ Dynamics in Astrocytes

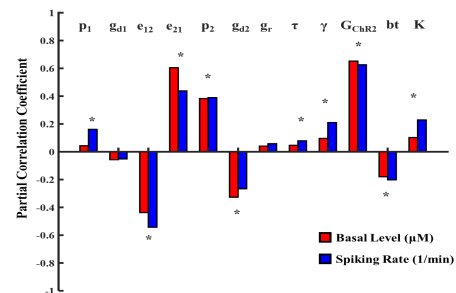
**Authors:** Lakshmini Balachandar, Karla A. Montejo, Arash Moshkforoush, Carolina Moncion, Eleane Castano, Melissa Perez, Jorge Riera Diaz

**Faculty Advisor:** Jorge Riera Diaz, Ph.D.

Targeted excitation of astrocytes via modulation of calcium ( $\text{Ca}^{2+}$ ) oscillations using a technique like optogenetics can prove to be crucial in therapeutic intervention of a variety of neurological disorders. However, a systematic study quantifying the effect of optogenetic stimulation in astrocytes is lacking. We use live brain slices from a knock-in mouse model expressing Channelrhodopsin 2 (ChR2) in cortical astrocytes to quantify  $\text{Ca}^{2+}$  responses in response to stimulation. We have developed and standardized a protocol for brain tissue extraction, vibratome sectioning,  $\text{Ca}^{2+}$  indicator loading, maintenance of slice health and  $\text{Ca}^{2+}$  imaging during light stimulation. Upon stimulation with different light paradigms, cortical astrocytes exhibited varying patterns of  $\text{Ca}^{2+}$  activity qualitatively different with respect to glutamate stimulation controls (Fig 1A-C). We employ a novel  $\text{Ca}^{2+}$  dynamics computational model to probe the optimal light stimulation paradigms necessary to elicit ideal astrocytic activity. Simulation revealed a consistent pattern of  $\text{Ca}^{2+}$  activity among individual cells in response to optogenetic stimulation, i.e., showing steady state regimes with increased  $\text{Ca}^{2+}$  basal level and spiking probability. Analysis of simulations allow us to identify significant kinetics that shape the calcium response (Fig 1D). Collectively, the framework presented in our study provides valuable information in the selection of paradigms that elicit optimal astrocytic activity using existing ChR2 constructs, as well as aid in the engineering of future optogenetic constructs.



Ex vivo  $\text{Ca}^{2+}$  imaging on the MIC – ChR2 knock-in mouse model. A. Time lapse of a recording with light stimulation from 180-220s; 200-250s; 300-400s and 480-530s. B. Overlay of the ChR2-EYFP (Green) construct with Rhod 2 AM (Red). C. Synchronized  $\text{Ca}^{2+}$  responses from various astrocytes firing upon light stimulation.



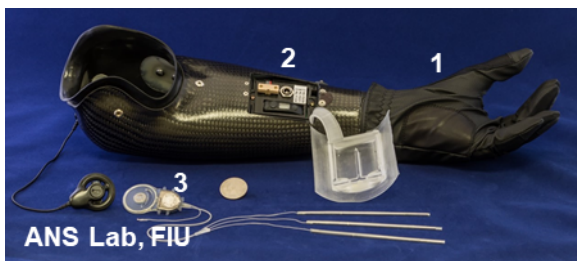
Global sensitivity analysis results depicting sensitivity of astrocyte  $\text{Ca}^{2+}$  activity to parameters of ChR2 during light stimulation - 50 s – end (total simulation time = 40 min, 10 trials) with respect to the basal level (nM) and spiking rate (1/min).

# Sensory Feedback Using a Neural Stimulation System with Longitudinal Intrafascicular Electrodes (LIFEs): A Long-Term study

**Authors:** Sathyakumar S Kuntaegowdanahalli, Anil Thota, James Abbas, Ranu Jung

**Faculty Advisor:** Ranu Jung, Ph.D.

Current state-of the art upper limb prosthesis systems lack sensory feedback. This deficiency increases the attentional demands of individuals with upper limb amputation as they perform activities of daily living and leads to reduced user satisfaction. Recent studies have shown that the existing neural feedback pathways in the residual limbs of individuals with amputation can be leveraged to restore sensation using direct neural stimulation of nerve fibers in the residual limb. Several sensory feedback systems have been developed using different electrode-nerve interface technologies. Some of the developed systems utilize electrodes implanted around peripheral nerves in the residual limb while others use electrodes implanted inside the fascicles in close proximity to nerve fibers. We have adopted the latter approach and developed the Neural Enabled Prosthetic Hand (NEPH) system to provide sensory feedback to individuals with amputation. The system includes a fully implantable neural stimulator with longitudinal intrafascicular electrodes (LIFEs) that are implanted in the peripheral nerves of the residual limb. An external processor maps sensor signals from the prosthetic hand to stimulation commands that are subsequently transferred to the stimulator through a wireless link. The NEPH system has been deployed in one person with transradial amputation for over 22 months with the subject using the device outside the lab for over 18 months. Electrode stability was evaluated by measuring electrode impedance, and minimum stimulation levels required to elicit percept. Additionally the utility of the sensory feedback provided by the system was evaluated using specially designed functional tasks. Results to date indicate that the intrafascicular neural interface of the NEPH system is stable and that the NEPH system can be used to provide functionally meaningful sensations that can be utilized by individuals with an upper extremity amputation to perform activities of daily living.



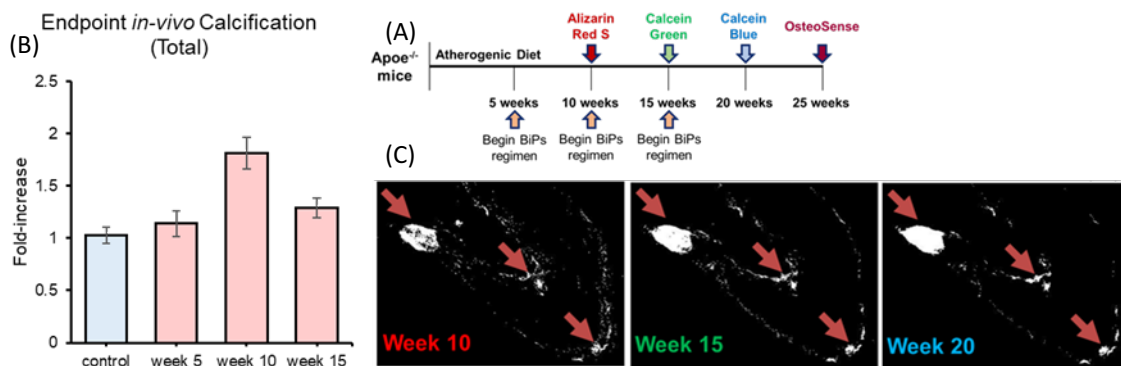
Fully assembled ANS-NEPH system and implant. 1) Instrumented Prosthetic Hand (IPH), 2) Implant Hand Interface 3) Implantable Stimulator Recorder (ISR) implant unit.

# Longitudinal In-Vivo Study on Bisphosphonate Treatment in Development of Vascular Calcification

**Authors:** Amirala Bakhshiannik, Valentina Dargam, Manuel Garcia Russo, Joshua Hutcheson

**Faculty Advisor:** Joshua Hutcheson, Ph.D.

Calcium mineralization occurs physiologically through bone formation and pathologically in cardiovascular calcification. Bisphosphonates are common osteoporotic therapeutics, which stabilize calcium phosphate mineral. They also prevent mineral growth and maturation in cardiovascular tissue by chelating phosphate ions that are required for calcification. However, administration of these therapeutics led to increased rates of cardiovascular incidents in patients with cardiovascular event history. In this study, we hypothesized that bisphosphonates exacerbate mineral formation if given once calcification has begun. We analyzed calcification growth over 25 weeks in Apolipoprotein E-deficient (Apoe<sup>-/-</sup>) mice on an atherogenic diet (42% fat). Vascular calcification has been previously observed after 10 weeks of atherogenic diet in these mice. Following 5, 10, or 15 weeks of the diet, the mice received biweekly subcutaneous injections of ibandronate sodium bisphosphonate (2 mg/kg). Tail-vein injections of calcium tracer dyes, namely Alizarin Red S, Calcein green, Calcein Blue, and near-infrared OsteoSense, were given after 10, 15, 20, and 25 weeks of the diet, respectively, to track the calcification at these time-points. Bisphosphonate treatment increased calcification in the aorta for groups treated after 10 and 15 weeks of the diet compared to the control group (biweekly saline injection) by 68 and 23 percent, respectively. We observed no change in the group treated after 5 weeks of the diet compared to the control group. In vivo data support our hypothesis that bisphosphonate promotes cardiovascular calcification if given after initial mineral nucleation. These studies could inform clinical decisions regarding potential cardiovascular effects of bisphosphonate treatment.



(A) Study Protocol; (B) Endpoint calcification measured using near-infrared OsteoSense; (C) Fluorescent calcium tracers to detect calcification longitudinally.

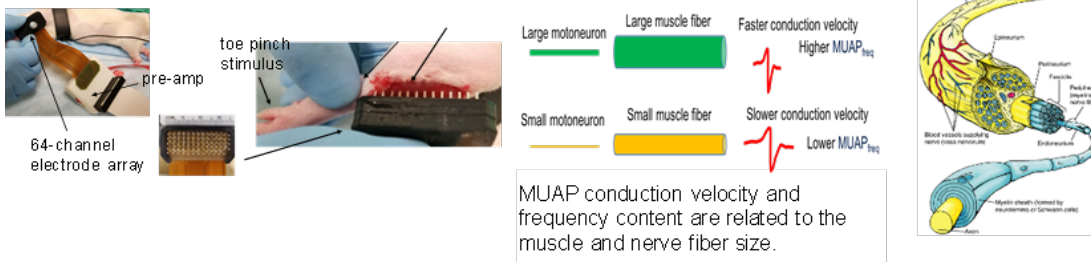


# Improving Nerve Fiber Selectivity on Intrafascicular Stimulation

**Authors:** Arianna Ortega, James J Abbas, Ranu Jung, Yannick Bornat, Florian Kölbl, Laura McPherson, Anil K, Thota, Olivier Romain, Sylvie Renaud

**Faculty Advisor:** Ranu Jung, Ph.D.

The network of peripheral nerves modulates and/or monitors the function of internal organs or the brain. Electrical stimulation of small groups of these nerves can form the foundation of bioelectronic systems to treat medical conditions such as spinal cord injury or limb loss. The anatomical organization of peripheral nerves, especially the fascicles centered within the nerve fibers, could be used for precise control of spatiotemporal patterns. Longitudinal intrafascicular electrodes (LIFEs) allow access to fibers in the fascicle and their mechanical properties are well-suited for chronic implantation. Electrical stimulation using LIFEs may enable activation with enhanced sub-fascicular selectivity using advanced stimulation strategies. In this project, the main objective is to improve selectivity of peripheral nerve fiber activation with LIFEs in the sciatic nerve of a rabbit. This objective will be tested using two variables: 1. employment of multiple electrode within the same fascicle for electric field steering and 2. changing the shape of the waveform of the stimulation pulse. In order to assess the ability achieve sub-fascicular selectivity high density EMG of the lower limb muscles will be recorded for motor unit action potentials (MUAP) and, kinematic and kinetic testing are performed. High frequency stimulation blocking will be applied to the nerve to identify the type of fiber and type of compound action potential (fast or slow) that is blocked. In addition, to characterize the conductivity of the nerve and electrode characteristics, the sciatic nerve will be extracted from the animal and placed in a PDMS mold, where 4 LIFEs are used in parallel. Several stimulations will be applied to measure the impedance. Supported by: RO1:EB027584.



Experimental set up for EMG recording and expected MUAPs.

Nerves morphology.

Ø Nerve: 2-4 mm

Ø Fascicle: 0.1-0.5 mm

Ø Axon: 0.2-20 µm

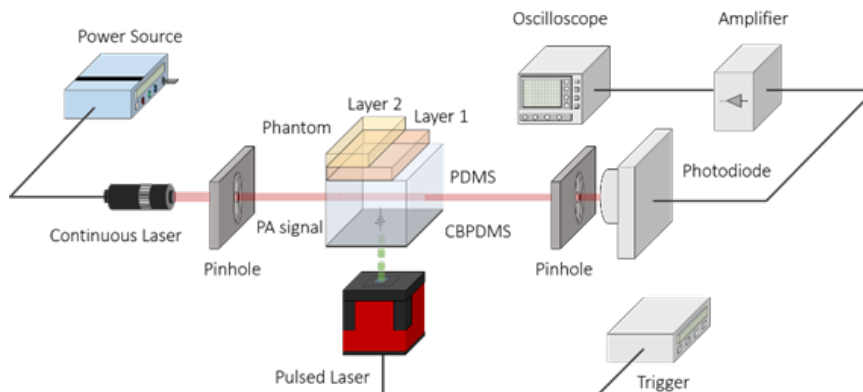
Moore and Dalley (2006).

# All-Optical Ultrasound System

**Authors:** Mohamed Almadi, Wei-Chiang Lin

**Faculty Advisor:** Wei-Chiang Lin, Ph.D.

In US imaging, lead zirconate titanate (PZT) transducers are commonly used to generate and detect ultrasound signals. However, this type of transducers has several major limitations such as susceptibility to electromagnetic interference, high driver voltage, and cross-talk among elements. For these reasons, it is complicated to design and miniaturize a PZT-based ultrasound probe for biomedical applications. Over the recent past, the concept of using optical techniques to perform US imaging has been proposed and explored. This alternative approach eliminates the limitations posed by the PZT transducers. More importantly, it has been shown that optical ultrasound transmitters can provide a tunable central frequency and optical ultrasound detectors have the potential to maintain their sensitivity when miniaturized. These advantages together make optical-based ultrasound imaging well suited for various diagnostic applications in biomedicine. In this study, the development of a prototype all-optical-ultrasound -imaging (AOUSI) system is presented. The optical ultrasound transmitter in the prototype AOUSI system was designed using the photoacoustic theory; the optical ultrasound detector the laser beam reflectometry theory. The imaging capability of the prototype AOUSI system was successfully demonstrated using layered ultrasound phantoms. Future work will include testing the 3-D imaging capability and the quantitative ultrasound measurement capability of the AOUSI system.



The experimental setup to test all-optical ultrasound imaging system.



# Age-Related Reduction of Urethral Afferent Sensitivity

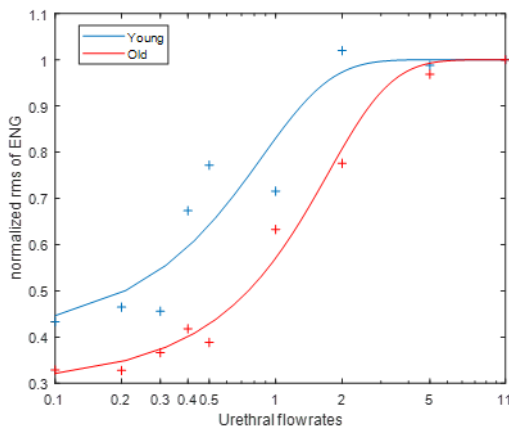
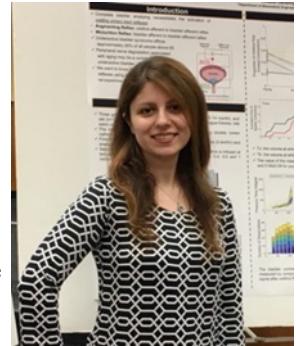
**Authors:** Arezoo Geramipour, Zachary Danziger

**Faculty Advisor:** Zachary Danziger, Ph.D.

Age-related underactive bladder (UAB) can lead to lower urinary tract (LUT) infection, yet the underlying causes of age-related UAB are still unknown. Complete bladder emptying requires the activation of voiding reflexes, and intact urethra afferent signaling is crucial to the normal function of urinary tract reflexes. The augmenting reflex is the activation of a reflex from the urethra afferents to the bladder efferent, which leads to a bladder contraction, and failure of this reflex disrupts the efficient voiding. In this study, we measure directly the urethral afferents to investigate if urethral signaling weakens with age and if this loss of sensitivity drives reduced reflex function.

We used urethane-anesthetized female Sprague–Dawley rats across their natural lifespan to quantify the effect of aging on the urethra afferents signaling. A catheter was passed through the intravesical space into the urethra to allow infusion of fluid through the urethra. The abdomen was sutured closed but we left the bladder incision open so that the bladder remained empty during the experiment. The pudendal nerve was exposed and the sensory branch was isolated from the compound nerve and connective tissue. A bipolar nerve cuff electrode was placed on the sensory branch of the pudendal nerve and at 2 minute intervals the urethra was infused at a pseudorandomly selected flow rates to compare the urethra afferents response to a range of urethra flow rates in different animal age groups.

Results show that urethra afferent signaling is weaker in older animals. The sensitivity of urethra afferents to urethral flow was shifted to higher flow rates with age, indicating that higher flow rates are required in older animals to recruit the urethra afferents. Therefore, the signaling reduction of urethra afferents to flow may weaken the augmenting reflex activation and contribute to incomplete bladder emptying in elderly population.



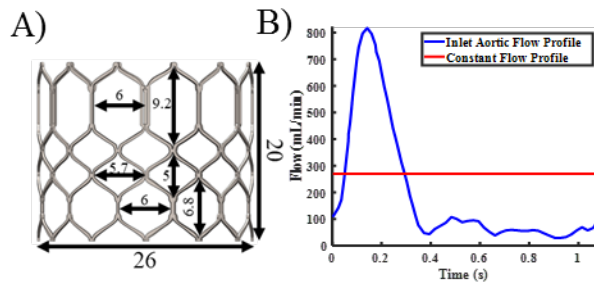
The sensitivity of urethra afferents to flow decreases with age.

# Fluid Dynamics on a Edwards Sapien 3 Stent and Its Implications to Thrombosis

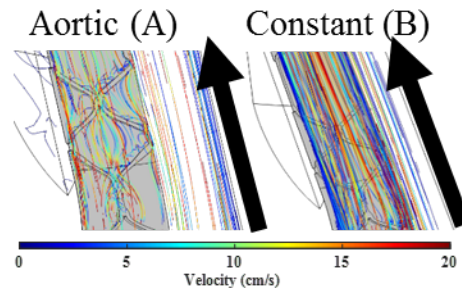
**Authors:** Asad M. Mirza, Amanda Barreto, Sharan Ramaswamy

**Faculty Advisor:** Sharan Ramaswamy, Ph.D.

Trans-aortic valve replacement (TAVR) procedures have become popular for treatment of calcified aortic valve disease (CAVD). However, this device is prone to thrombosis, leading to progression to stroke. It has been previously shown that flow stagnation, low wall shear stress (WSS), and high oscillatory shear stress (OSS) correlate with thrombosis formation. Our objective was to identify a link between blood flow pulsatility and risk for thrombosis, i.e., clot formation by examining the hemodynamic environment surrounding the stent of a commercially-available TAVR system SAPIEN 3. A 26 mm SAPIEN 3 stent geometry was modeled in Solidworks 2020. The stent was placed in a mimicked adult aortic geometry. Blood was assumed to be incompressible and its viscosity was defined using the non-Newtonian Carreau model. Two simulations (COMSOL Multiphysics with ANSYS Meshing) were done, one with a physiologically relevant aortic inlet flow profile and another with its average. For the aortic flow-case, peak velocity streamlines showed more disturbed flow surrounding the TAVR stent-region. The constant flow case was unidirectional with mild to no flow disturbances near the stent-struts. Overall, the TAWSS on the stent was low for the aortic flow-case, <4 dynes/cm<sup>2</sup>, and even lower for the constant flow case. Fluid-induced oscillatory shear stresses were found under the aortic pulsatile flow condition, but none were present for constant flow case. We report that blood pulsatility induces a high degree of temporal blood oscillations on TAVR stents-geometries-alone, specifically at the distal strut surfaces, potentially making these locations vulnerable to clot formation.



Pre-Simulation Setup A) Edward's SAPIEN 3 CAD geometry, all units are in mm. B) Inlet boundary flow profiles, aortic flow (blue) and its average (red).



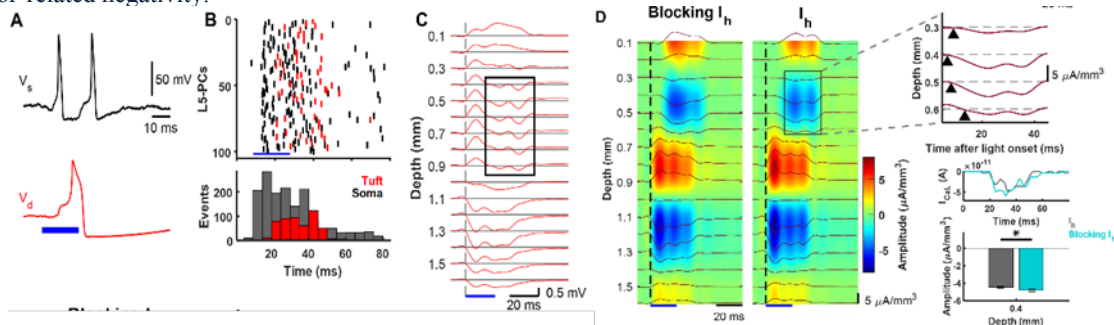
Simulation results on a portion of the stent showing velocity streamlines with flow arrow direction under two conditions, aortic (A) and constant (B) flow.

# A Minimal Biophysical Model of Neocortical Pyramidal Cells: Implications for Frontal Cortex Microcircuitry and Field Potential Generation

**Authors:** Beatriz Herrera, Amirsaman Sajad, Geoffrey F. Woodman, Jeffrey D. Schall, Jorge Riera Diaz

**Faculty Advisor:** Jorge Riera Diaz, Ph.D.

$\text{Ca}^{2+}$  spikes initiated in the apical dendrites of layer-5 pyramidal cells (PC) underlie nonlinear dynamic changes in the gain of cellular response, which is critical for top-down cognitive control. Detailed models with several compartments and dozens of ionic channels have been proposed to account for this  $\text{Ca}^{2+}$  spike-dependent gain with its associated critical frequency. However, current models do not account for all known  $\text{Ca}^{2+}$ -dependent features. Previous attempts to include more features have required increasing complexity, limiting their interpretability and utility for studying large population dynamics. We present a minimal 2-compartment biophysical model, overcoming these limitations. In our model, a basal-dendritic/somatic compartment included typical  $\text{Na}^+$  and  $\text{K}^+$  conductances, while an apical-dendritic/trunk compartment included persistent  $\text{Na}^+$ , hyperpolarization-activated cation ( $I_h$ ), slow inactivation  $\text{K}^+$ , muscarinic  $\text{K}^+$ , and  $\text{Ca}^{2+}$  L-type. The model replicated the  $\text{Ca}^{2+}$  spike morphology and its critical frequency plus three other defining features of layer-5 PC synaptic integration: linear frequency-current relationships, backpropagation-activated  $\text{Ca}^{2+}$  spike firing, and a shift in the critical frequency by blocking  $I_h$ . Simulating 1,000 synchronized layer-5 PCs, we reproduced the current source density patterns evoked by  $\text{Ca}^{2+}$ -spikes both with and without  $I_h$  current. Thus, a 2-compartment model with five non-classic ionic currents in the apical-dendrites reproduces all features of these neurons. We discuss the utility of this minimal model to study the microcircuitry of agranular areas of the frontal lobe involved in cognitive control and responsible for event-related potentials such as the error-related negativity.



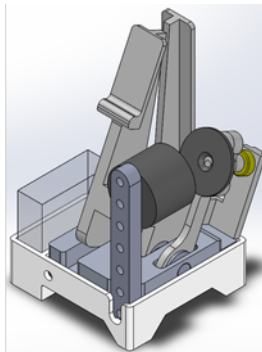
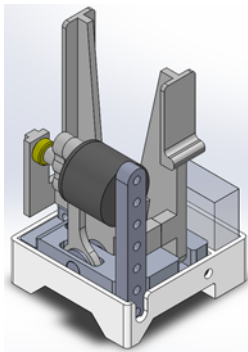
LFP and CSD derived from dendritic  $\text{Ca}^{2+}$ -spikes in a collection of L5-PCs. A. Somatic (black) and apical-dendritic/trunk (red) simulated responses of a neuron. B. Raster plots (top) and post-stimulus time histogram (bottom) of 100 randomly selected L5-PCs (top). C. LFPs evoked by the collection of L5 PCs. D. CSD analysis of the evoked LFPs without (left) and with (right) the  $I_h$  current. Middle right panel plots averaged  $I_{CaL}$  current in the trunk of the L5-PCs. Blue bar: stimulation window.

# Design of a Fragile Object Simulator for the Assessment of Sensory Feedback Utility During Functional Tasks

**Authors:** Diego Aguilar, SS Kuntaegowdanahalli, James Abbas, Ranu Jung

**Faculty Advisor:** Ranu Jung, Ph.D.

Without the sense of touch, upper-limb amputees using a hand prosthesis struggle to handle fragile objects. Fragile objects require fine control of hand motions to avoid crushing or dropping them. Systems like the Neural-Enabled Prosthetic Hand (NEPH) provide sensory feedback to the amputee about the state of their prosthetic hand. Tests are needed to validate the impact of sensory feedback on the subject's performance while operating their prosthetic hand. Psychophysical tests involving functional tasks provide conditions that mimic activities of daily living, where the subject can use their neural-enabled prosthesis to perform familiar hand motions and experimenters can observe changes in performance. Object grip requires a level of motor control that will allow the subject to retain the object in their hand without slipping or crushing. It is challenging to obtain reliable repeatability while testing for the control of grip force because test objects must be replaced often. An experimental apparatus was designed to provide experimenters with a testing object that can simulate the mechanical behavior of a fragile object during a grip test. User requirements were collected from literature and experimenters, and concepts were explored in several prototyping cycles using 3D modeling and printing. The resulting Fragile Object Simulator (FOS) measures the grip force applied to it by an electromechanical prosthetic hand and collapses once the force has reached a threshold. The collapse is reversible with no damage to the assembly, and the threshold is specified by the experimenter. This experimental apparatus provides a reusable test object with repeatable physical characteristics that can be adjusted to the objectives of the experiment. The FOS prototype will undergo validation testing with the objective of incorporating it into clinical trials involving the NEPH system.



Fragile Object Simulator  
mechanical model

# Magnetic Particle Enzyme Integrated Fluidic Sensing Platform

**Authors:** Lin Tong, Joshua Hutcheson

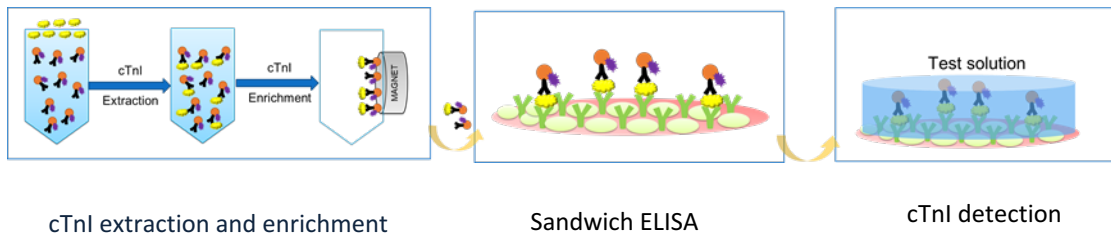
**Faculty Advisor:** Joshua Hutcheson, Ph.D.

Cardiovascular disease (CVD) is leading cause of death in the world. Cardiac Troponin I type (cTnI) has become the gold standard lab test for acute cardiac events, such as heart attacks, acute coronary syndrome, and unstable angina. However, the high cost and time consuming nature of associated assays for cTnI limit its applicability for underserved populations.

One goal of the NSF-sponsored Precise Advanced Technologies and Health Systems for Underserved Populations (PATHS-UP) Engineering Research Center is to develop a cost-effective point of care device for cTnI monitoring and detection.

Our proposed detection method for cTnI includes a magnetic particle based sample extraction and enrichment followed by detection using a modified sandwich enzyme-linked immunosorbent assay method. Invertase is used to convert the signal from nM levels of cTnI to mM levels of glucose. A colorimetric paper pad is then used to quantify the glucose levels as a surrogate measure of cTnI concentration.

Using our current prototype, we can detect cTnI in a range from 1 to 100 ng/mL with an average standard deviation of 8.06 ng/ml. The ultimate goal of our technology is to detect cTnI at a clinically relevant concentration of 0.03ng/mL.



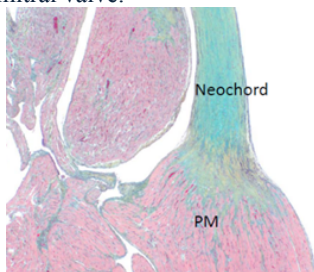


# Complete Regeneration Of Neochordae Component Of Bio-scaffold Mitral Valve Apparatus In A Non-human Primate Model

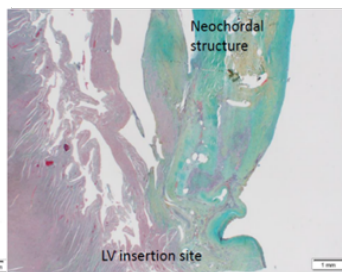
**Authors:** Brittany A. Gonzalez, Frank Scholl, Steven Bibeovski, Krishna Rivas Wagner, Jennifer Bibeovski, Lazaro Hernandez, Elena Ladich, Vincent Brehier, Mike Casares, Pablo Morales, Jesus Lopez, Joseph Wagner, Sharan Ramaswamy

**Faculty Advisor:** Sharan Ramaswam, Ph.D.

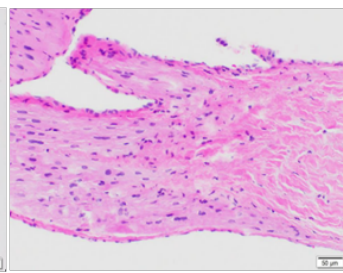
Congenital heart defects (CHDs) are the most common type of birth anomaly, affecting 8 out of 1,000 newborns; each year about 35,000 babies in the United States are born with these defects. CHDs occur when there is a problem with the structure of the heart at birth, or soon after. Critical congenital heart valve defects (CCHVDs) are a subset of CHDs, which account for ~25% of all CHD cases. Timely treatment plays a key role in CCHVDs. However, CCHVDs in newborns have very limited treatment options due to challenges associated with the unavailability of small-sized commercial valves and the inability of prosthetic valves to support somatic growth. To facilitate growth, we successfully implanted a bioscaffold valve comprising of porcine small intestinal submucosa (PSIS) in an animal model to assess de novo tissue formation over time post-implantation. Juvenile baboons (12-14 months, n=3) were implanted with a hand-made bicuspid tubular-shaped, PSIS (Cormatrix, Roswell, GA) valve in the mitral position. The PSIS valves were explanted at 11-month and 20-month post-implantation for histological assessment via hematoxylin and eosin (H&E) and Movat's Pentachrome (Movat's) staining via Alizée Pathology, Inc. manufacturing protocol. It was found that at both time points (11- and 20-month explants) that PSIS was able to regenerate neochordae, composed of collagen and proteoglycans. Our findings suggest that our PSIS bioscaffold can regenerate a neochordae and integrate well with the papillary muscle, as well as the left ventricle without any need to biochemical or biomechanical treatment or stimulation. Nonetheless, to enable a successful bio-scaffold mitral valve apparatus with regenerative capacities, it is important to assess other components of the PSIS mitral valve.



PSIS mitral valve explant at 11-month post-implantation. Neochordal structure with papillary muscle (PM) insertion site.



PSIS mitral valve explant at 20-month post-implantation. Neochordal structure with left ventricle (LV) insertion site.



PSIS mitral valve explant at 20-month post-implantation. Neochordal structure with a collagenous core with cell infiltration; endothelial cells are covering the surface.

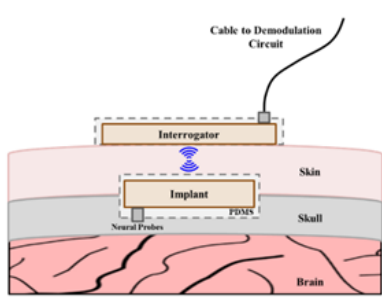
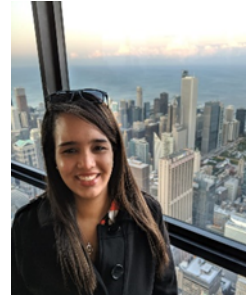


# Recording Multiscale Neural Activity Using Wireless Neurosensing System

**Authors:** Carolina Moncion, Lakshmini Balachandar, Diana Borrego, Satheesh Bojja-Venkatakrishnan, Asimina Kiourti, John L. Voalkis, Jorge Riera Diaz

**Faculty Advisor:** Jorge Riera Diaz, Ph.D.

A unique system, namely the wireless neurosensing system (WiNS) is tested, for the first time, in a freely moving animal. WiNS was designed to sense neural signals in a battery-free manner, without using complex electronics, and by integrating the key components: (a) implant and external interrogator, (b) neural probes, and (c) demodulation circuit (see Fig. 1a). Here, a set of in vivo experiments are carried out to demonstrate recovery of neural signals associated with transitions among states of awareness, and while alternating between resting and walking. These first ever results were made possible by (a) newly developed low-impedance neural probes to closely match the impedance of WiNS and (b) realization of a new custom 3D printed cap (see Fig. 1b). To further advance towards our end goal, of multiscale neural recordings with WiNS, we adapt it with an impedance matching network. This adapted version was then applied to record spontaneous neural unit activity from the hippocampus of a Wistar rat. Collectively, the recorded signals provide concrete proof of this technology's pertinent role in neuroscience.



(a)



(b)

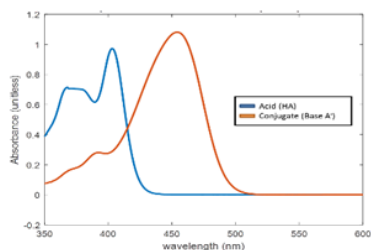
Wireless Neurosensing System (WiNS). (a) Intended implementation of WiNS with each of the key components highlighted. (b) External stereotaxic cap used to perform freely-moving recordings.

# Implantable Carbon Dioxide Sensor for Subcutaneous Capnography

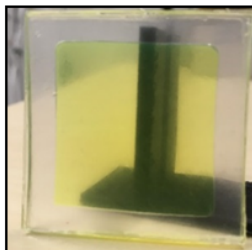
**Authors:** Teshaun J. Francis, Wei-Chiang Lin

**Faculty Advisor:** Wei-Chiang Lin, Ph.D.

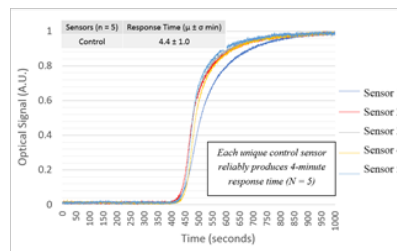
The ultimate objective of this project is to design an implantable carbon dioxide sensor capable of estimating arterial carbon dioxide tension ( $\text{PaCO}_2$ ) from interstitial carbon dioxide tension ( $\text{iCO}_2$ ). In pursuit of this goal, an optochemical  $\text{CO}_2$  sensor was designed, fabricated, and characterized on the benchtop. The sensor design was based on the optochemical Severinghaus implementation, which measures  $\text{CO}_2$  as a function of pH; fabrication was done in-house. The  $\text{CO}_2$ -sensing solution was comprised of 8-Hydroxypyrene-1,3,6-Trisulfonic Acid, Trisodium Salt (HPTS) as the optical pH indicator dye, sodium bicarbonate ( $\text{NaHCO}_3$ ) as a basic buffer, and deionized water. HPTS has strong absorption in the visible wavelength region and the  $\text{pK}_a$  value of HPTS is near-neutral (i.e. 7.3) which makes it ideal for  $\text{CO}_2$ -sensing on the benchtop. The molar absorbance coefficients of the acid and conjugate base (HA and A<sup>-</sup>, respectively) were characterized experimentally using a spectrophotometer (i.e., Figure 1). The dye solution used in this study contained 1 mM of  $\text{NaHCO}_3$  and 150  $\mu\text{M}$  HPTS. Prototype optochemical  $\text{CO}_2$  sensors were constructed entirely of polydimethylsiloxane (PDMS). Dye solution was injected directly into the center of the structure (i.e. Figure 2). Characterization was performed on a custom-built system for simultaneous gas-control and optical spectroscopy. Light transmission through the sensor was monitored continuously as a step change in  $\text{CO}_2$  was applied, to produce an optochemical response curve (i.e. Figure 3). Sensor thickness was identified as a critical factor controlling response time, so an experimental validation was carried out to confirm this finding. Compared to the control sensors, sensors with thicker selective membranes possessed a significantly slower response time ( $p < 0.05$ ). However, sensors with thicker sensing media showed an average response time similar to that of the control sensors. These results demonstrate the feasibility and capability to develop an optochemical  $\text{CO}_2$  sensor and illuminate strategies for optimization.



The pH-dependent absorbance spectrum of the pH indicator dye.



Proof-of-concept optochemical  $\text{CO}_2$  sensors



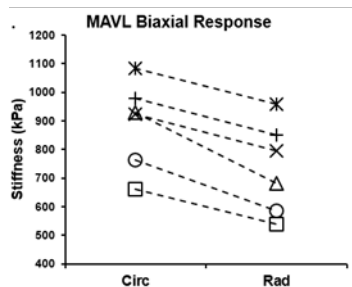
The effect of layer thickness on the response time of the optochemical  $\text{CO}_2$  sensor.

# A Method to Quantify Tensile Biaxial Properties of Mouse Aortic Valve Leaflets

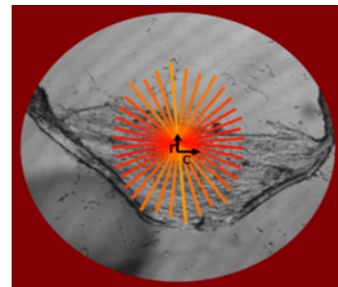
**Authors:** Daniel Chaparro, Valentina Dargam, Paulina Alvarez, Jay Yeung, Ilyas Saytashev, Jenniffer Bustillo, Archana Loganathan, Jessica Ramella-Roman, Arvind Agarwal, Joshua Hutcheson

**Faculty Advisor:** Joshua Hutcheson, Ph.D.

The aortic valve (AV) has a highly organized extracellular matrix (ECM) in which orthogonally aligned collagen and elastin fibers allow it to open and close over 3 billion times in an average lifetime. AV disease is characterized by asymptomatic pathological remodeling of the ECM leading to improper valve function. Various animal models are used to characterize and understand human aortic valve disease. Large mammals have been used extensively to assess the relation between structural macromolecular ECM components and the mechanical properties of the tissue elucidating the importance of these components in AV function. Smaller mammals, on the other hand, are used in mechanistic studies as they can be genetically modified to recapitulate certain aspects of human aortic valve disease. Combining mechanical strain regimen and biological mechanistic studies is a major obstacle for both large and small mammals since large mammals are expensive to genetically modify and small mammal tissues are difficult to mechanically test. Mouse aortic valve leaflet (MAVL) tensile properties have not been properly quantified due to their microscopic size (500  $\mu\text{m}$  long and 50  $\mu\text{m}$  thick). In this study, we developed a method in which the biaxial tensile properties of MAVL tissues can be assessed by adhering the tissues to a silicone rubber membrane. Applying equiaxial tensile loads on the tissue-membrane composite and tracking the engineering strains on the surface of the tissue resulted in the characteristic orthotropic response of AV tissues seen in larger mammals. Our data suggests that the circumferential orientation, corresponding to the preferential alignment of collagen fibers, is approximately 155 kPa stiffer than the radial orientation ( $n=6$ ,  $P=0.0006$ ) in MAVL tissues. This method can be implemented in future studies involving mechanical stimulation of genetically modified MAVL tissues bridging the gap between biomolecular mechanisms and valve mechanics in mouse models of valve disease.



Comparison of MAVL stiffness in the radial and circumferential strain directions are significantly different (paired t-test, two-tailed, 95% CI,  $p < 0.05$ ).



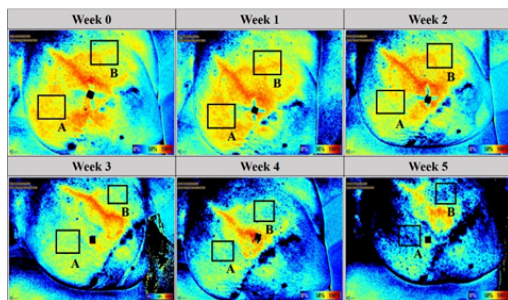
Representative direction dependent strain field on the surface of a mouse aortic valve leaflet under strain. The radial (r) and circumferential (c) directions are depicted.

# Tissue Oxygenation as a Biomarker for Radiation Dermatitis in Radiation-Therapy Treated Breast Cancer Subjects

**Authors:** Edwin A. Robledo, Kevin Leiva, Juan Murillo, Corina E. Beiner, Maria Amelia Rodrigues, Joseph Panoff, Marcio Fagundes, Michael Chuong, Anuradha Godavarty

**Faculty Advisor:** Anuradha Godavarty, Ph.D.

For many patients undergoing radiation therapy (RT), radiation dermatitis (RD) is an expected adverse treatment-related effect. The American Cancer Society has estimated that a total of 1.8 million new cancer cases will arise in 2020, 15% percent of which are breast cancer. Acute RD ranges from mild erythema to dry and moist desquamation, which is a significant cause of treatment-related morbidity including pain and psychological distress. Current assessment of RD is mostly subjective, requiring visual inspection by a clinician, which can differ from person to person. This leads to misinformed treatment plans and mismanagement of RD. The Optical Imaging Laboratory (OIL) at FIU is working toward a method to characterize RD by employing an NIR spectroscopy (NIRS) based imaging technique to map the spatial and temporal changes in tissue oxygenation in breast cancer subjects. Optical techniques have been employed in the past by several research groups in order to characterize the severity of RD and predict the onset of RD using several biomarkers. It was seen in several animal model studies that tissue oxygenation ( $\text{StO}_2$ ) could observe changes in response to radiation sooner than visual changes, allowing  $\text{StO}_2$  to serve as an early detection biomarker of skin toxicity. A WIRB approved longitudinal pilot study was launched in collaboration with Miami Cancer Institute (MCI). 10 breast cancer patients were consented to participate in the study. Imaging took place weekly throughout their RT treatment. Preliminary results from the ongoing study have shown that there are distinct changes (decrease) in oxygen saturation with increase in severity of RD (or skin toxicity). Further analysis is required to correlate the results to severity of RD. Characterizing the severity of RD using a functional biomarker such as tissue oxygenation can lead to objective diagnosis and prevention of RD. Clinicians can standardize treatment plans based on the analysis of oxygenation levels around regions of interest during RT.



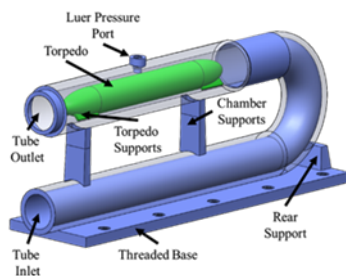
Oxygen saturation ( $\text{StO}_2$ ) maps acquired using Kent's SnapshotNIR during weeks 0 through 5 of Radiotherapy of one subject's left breast. A fiducial marker was placed near the center of the region of interest to easily compare between multiple images.

# Torpedo-Shaped Bioreactor Design for Tubular Heart-Valve Bioscaffold

**Authors:** Manuel Perez-Nevarez, Brittany Gonzalez, Asad Mirza, Marcos Gonzalez, Sharan Ramaswamy

**Faculty Advisor:** Sharan Ramaswamy, Ph.D.

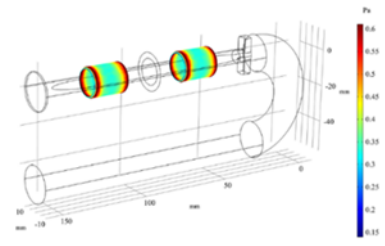
Tissue engineered heart valve (TEHV) constructs have been studied as replacement for diseased or dysfunctional heart valves. Porcine small intestinal submucosa (PSIS) decellularized tissue has been previously evaluated as implant material to replicate heart valve function. Ideally, TEHV are intended to integrate into the native somatic tissue. To achieve this, we have previously seeded PSIS with Bone Marrow Stem Cells (BMSC) with the aim of achieving de novo extracellular matrix production and integration into native tissue. Our previous tissue engineering bioreactor studies have shown that flow-induced shear stress can influence vascular phenotype development and tissue formation. Flow-conditioning bioreactors have been designed to replicate physiologically relevant shear stresses and oscillatory shear forces experienced by native vascular tissue. We have developed a 2nd generation bioreactor system that can include provisions for the mechanical conditioning of tubular-shaped PSIS scaffolds (Figure 1). The system includes a torpedo-shaped sample holder that was designed to accommodate two cylindrically-shaped tubular scaffolds (Figure 2) while retaining the ability to produce physiologically relevant hemodynamic shear forces over the scaffold surfaces. The dimensions of the bioreactor chamber were selected to maintain relevant shear stress forces over the scaffold surfaces (Figure 3). This serves to subject the tubular PSIS specimens to sinusoidal flow and pressure variations produced by heart pulsation during its heartbeat. Our overall objective is the design a bioreactor system that can generate implantable tissues by conditioning BMSC seeded PSIS scaffolds to promote tissue formation and subsequently produce TEHV constructs that can be then implanted in vivo.



Bioreactor System overview



Cylindrical PSIS scaffolds mounted on sample holder of Torpedo Bioreactor



Time-Averaged Wall Shear Stress

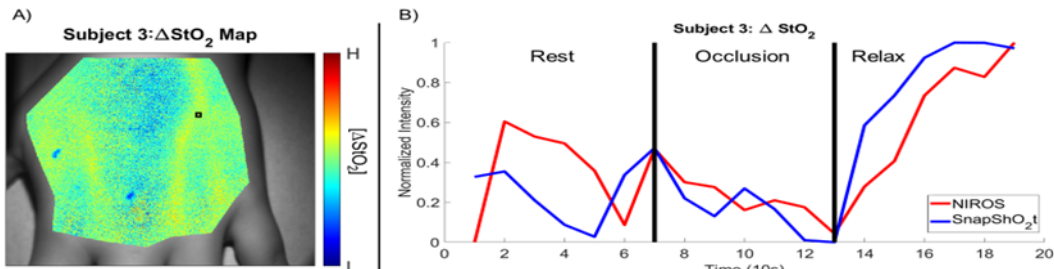


# In-Vivo Validation of a Near-Infrared Optical Scanner (NIROS) via an Occlusion Paradigm

**Authors:** Kevin Leiva, Edwin Robledo, David Ortega, Anuradha Godavarty

**Faculty Advisor:** Anuradha Godavarty, Ph.D.

Diabetic Foot Ulcers (DFU) affect approximately 25% of diabetics throughout their life. Adequate oxygen supply is crucial towards wound healing, yet the gold standard in assessment remains visual inspection of the wound. At the Optical Imaging Laboratory, we have developed a hand-held, Near InfraRed Optical Scanner (NIROS) to conduct static, non-contact, wound imaging to produce 2D tissue oxygenation (TO) maps. Recently, dynamic imaging capabilities were incorporated into the device to monitor TO changes across time. In this pilot study, the capability of NIROS to obtain spatial-temporal maps of TO changes, as a response to a hemodynamic stimulus, was assessed using an occlusion paradigm and validated with a commercial Near-Infrared Spectroscopy (NIRS) device. Three healthy normal subjects were recruited and sequentially imaged by NIROS and the commercial device at 1Hz and 0.1 Hz respectively. A three-minute occlusion paradigm, with 60 seconds of total occlusion, was utilized. In NIROS, the data was extracted at matched timepoints to the commercial device. Modified Beer-Lambert Law (mBLL) was utilized to calculate the effective TO in terms of Oxy- ( $\Delta\text{HbO}$ ), Deoxy- ( $\Delta\text{HbR}$ ), Total Hemoglobin ( $\Delta\text{HbT}$ ), and Oxygen Saturation ( $\Delta\text{StO}_2$ ). In the commercial device, the data was processed internally to produce  $\Delta\text{StO}_2$  maps. A region of interest (ROI) was selected at equivalent regions and binned across time to produce  $\Delta\text{StO}_2$  trendlines. The Pearson's Correlation Coefficient (PCC) between the devices was then calculated for each subject. Preliminary results indicate that both devices were able to detect changes in TO in terms of the  $\Delta\text{StO}_2$ . A decrease in  $\Delta\text{StO}_2$  was observed during occlusion followed by a sharp increase upon cessation, with high correlation between both devices from occlusion onset onward ( $>87\%$ ). The preliminary results described herein provide evidence of NIROS's ability to detect changes in TO via a hemodynamic stimulus.



A) StO<sub>2</sub> map for subject 3 with ROI demarcated by a black box. B) Normalized StO<sub>2</sub> trendline from NIROS (red) and the commercial device (blue).

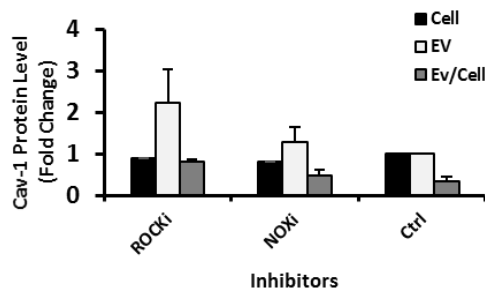


# NADPH Oxidase and RHO Kinase Modulate Caveolin-1 Release in Extracellular Vesicles from Vascular Smooth Muscle Cells under Mechanical Stretch

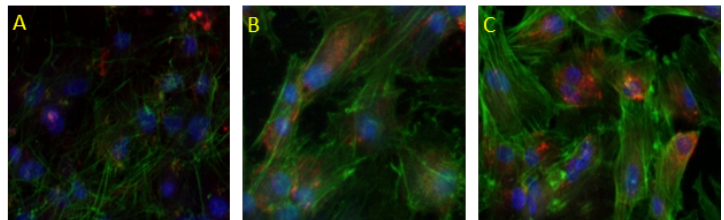
**Authors:** Mohammad Shaver, Joshua Hutcheson

**Faculty Advisor:** Joshua Hutcheson, Ph.D.

Extracellular vesicles (EVs) mediate intercellular trafficking and arterial wall remodeling. Caveolin-1 (Cav-1), a structural component of caveolae, plays a critical role in biogenesis of a subset of EVs from vascular smooth muscle cells (VSMCs) and is required for vascular calcification. Caveolae buffer the plasma membrane to changes in mechanical tension and actively participate in mechanotransduction. However, the effect of mechanical stretch on Cav-1-dependent EV formation in VSMCs remains unknown. In this study, porcine VSMCs were cultured under cyclic stretch (10%, 0.5Hz) for 72hrs. Western blotting showed a redistribution of Cav-1 into EVs ( $100\pm 25\%$  increase in the ratio of EV Cav-1 to intracellular Cav-1 for stretched VSMCs compared to non-stretched VSMCs) and a 55.1% reduction in smooth muscle alpha-actin in stretched VSMCs compared to non-stretched VSMCs. In order to investigate the role of the actin cytoskeleton in the stretch-induced Cav-1 trafficking, we inhibited Rho kinase ( $10\mu\text{M}$  Y-27632) and Nox1/4 ( $10\mu\text{M}$  GKT137831), mediators of VSMC actin filament dynamics. Compared to non-treated stretched samples, VSMCs under stretch treated with either inhibitor exhibited a further increase in Cav-1 redistribution to EVs ( $159\pm 38\%$  and  $60\pm 15\%$  increase in EV Cav-1/intracellular Cav-1 for Rho kinase inhibitor (ROCKi) and NOX1/4 inhibitor (NOXi), respectively, compared to VSMCs under stretch with no inhibitors). Immunofluorescence staining showed that both inhibitors reduced actin filaments and resulted in Cav-1 internalization within the VSMCs. Alterations in VSMC actin results in Cav-1 intracellular trafficking and EV release. These data provide new insight into the effect of mechanical stimulation on EV formation.



Values of caveolin-1 within the SMCs in comparison with the extracellular.



Immunofluorescent images of SMCs exposed to cyclic stretch and treated with ROCKi (A), NOXi (B) and non-treated control SMCs (C).

# A Non-Contact Smartphone-Based Near Infrared Scanner to Measure Tissue Oxygenation

**Authors:** Kacie Kaile, Christian Fernandez, Anuradha Godavarty

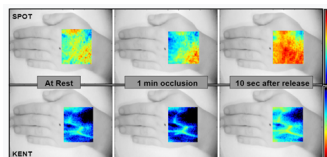
**Faculty Advisor:** Anuradha Godavarty, Ph.D.

Standard wound care management includes topical agents, bandages, and debridement of necrotic tissue to prevent infection. In healthy subjects, wounds progress through the usual stages of cell proliferation and reconstruction. However, for subjects with pre-existing conditions the healing process can be stalled for prolonged periods.

Conventional diagnostic methods include wound size and depth measurements while newer methods employ optical imaging. Diffuse optical imaging of wound beds using near infrared (NIR) light can determine subsurface changes in tissue oxygenation (TO). Low cost, portable imaging devices have been developed recently such as NIROS and KENT. As a next step to further mobilize this technology, smartphone based imaging is explored. Recently, a non-contact smartphone based NIR optical device was developed. The SmartPhone Oxygenation Tool (SPOT) measures 2D spatio-temporal TO maps. Preliminary in-vivo studies demonstrated the ability of this device to observe changes in diffuse reflectance in response to occlusion. The SPOT device in itself consists of the add-on module, smartphone, and app for acquisition and storage. The objective of this study is to validate changes in TO as detected by SPOT compared with a commercial imaging device, KENT. In this on-going study, one subject was recruited and imaged using SPOT device during a standard occlusion paradigm and sequentially using a commercial device. The oxygen saturation reduced upon a 1-min occlusion compared to rest conditions and increased significantly upon release (obtained 10-sec after). A similar trend of a decrease in oxygen saturation in response to occlusion and an increase upon release was observed using the commercial device. Ongoing efforts are in developing noise removal methods to enhance vasculature and quantify the extent of changes as measured by SPOT. NIR optical imaging using smartphone is achieved via add on source tool to illuminate tissue, capture multi-wavelength images, and obtain TO maps. Studies are ongoing on a statistically powered sample size in order to validate SPOT's ability to capture spatio-temporal physiological maps of tissues as a non-contact, compact, hand-held imaging device. The proposed SPOT system is a low-cost addition to wound care management with far-reaching (global) accessibility for a variety of clinical, in-home, and on-field settings.



App features LED & camera controls to allow for simultaneous illumination and detection, displays distance information from time-of-flight sensor and stores multi-wavelength images.



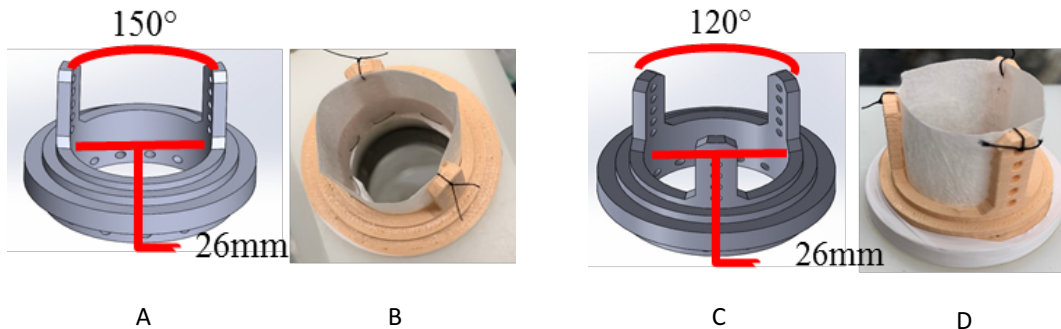
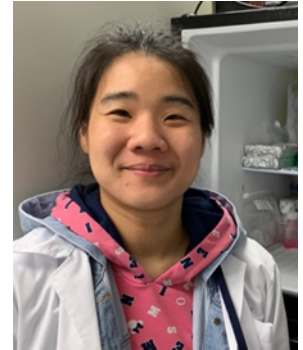
Oxygen saturation maps of the dorsal of the hand during (i) rest, (ii) 1-min after occlusion and (iii) following release of occlusion as measured by SPOT (top row) and KENT's device (bottom row).

# Hydrodynamic Assessment of a Small Intestinal Submucosa Tubular Valves

**Authors:** Chia-Pei Denise Hsu, Asad Mirza, Robert Matheny, Joshua Hutcheson, Sharan Ramaswamy

**Faculty Advisors:** Joshua Hutcheson, Ph.D.; Sharan Ramaswamy, Ph.D.

For children with critical valve defects and older patients who are contraindicated for receiving mechanical and bioprosthetic valves, treatment options are extremely limited. The purpose of this study is to determine whether tubular porcine small intestinal submucosa (PSIS) bio-scaffold valves can facilitate robust aortic and mitral valvular hydrodynamic functions and serve as potential treatment options. 26-mm PSIS tubular valves (CorMatrix Cardiovascular Inc., Roswell, GA) were sutured to a custom, 3D-printed valve holder along its ring and posts on the distal end. Three posts at 120 degrees apart were used for the aortic valve position, and two posts at 150 degrees apart were used for the mitral valve position. Hydrodynamic tests were performed using a pulse duplicator system (Vivitro Labs Inc., Victoria, Canada) filled with 0.9% saline solution. A flow probe was affixed between the aortic and ventricular chambers to measure the aortic outflow, and between the atrial and ventricular chambers to measure the mitral outflow. Three pressure transducers were inserted in the atrial, ventricular, and aortic locations. Tests utilized a stroke volume of 71.4 mL, 70 bpm, and an input flow waveform comprising of a 35% systolic-65% diastolic configuration (S35, Vivitest, Vivitro Labs). The tubular PSIS valves placed in both aortic and mitral positions appear to facilitate robust hydrodynamic valve function and may concomitantly serve as a scaffold for de novo valvular tissue growth by the host after implantation. Further studies involving seeding tubular PSIS valves with valvular cells and conditioning them in bioreactors will be conducted to assess the effects of both mechanical and biochemical stimuli on valve performance.



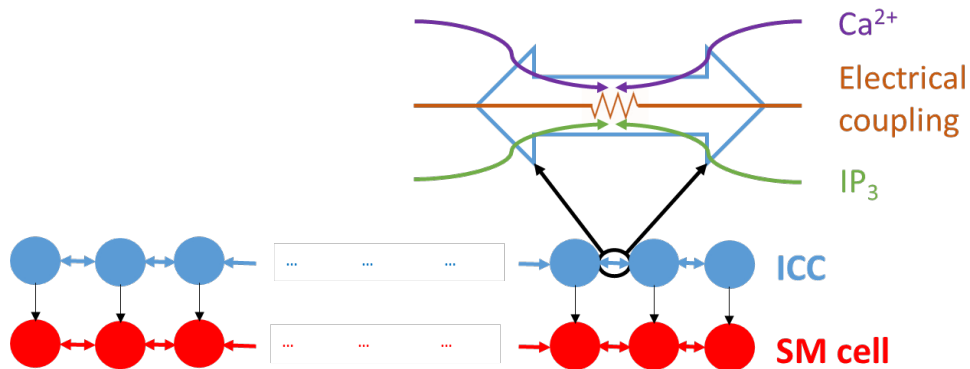
Cylindrical valves sutured onto customized valve holders (Mitral: A & B, Aortic: C & D), which are 3D printed with thermoplastic polyurethane (TPU) material.

# Modeling of an Entire Stomach: Are We Missing Something?

**Authors:** Ashfaq Ahmed, Ranu Jung

**Faculty Advisor:** Ranu Jung, Ph.D.

The stomach exhibits a characteristic slow wave of contraction. Slow waves originate from dominant pacemaker cells within the stomach wall along the greater curvature in the mid-corpus and spread aborally through the antrum to the pyloric sphincter. Disruption of the slow wave is supposed to play an active role in slowing down gastric motility. To better understand the mechanisms underlying slow wave anomalies, we have computationally modeled the slow waves as being generated by a chain of interconnected biophysical circuits of networks of cells. This biophysical circuit consists of interstitial cells of Cajal (ICC) and smooth muscle (SM) cells. The ICC have been modeled with a frequency gradient with the rostral most cell having the highest frequency and caudal most cell having the lowest frequency. In our initial model, ICC are electrically connected to each other through gap junctions and each SM cell is electrically connected to an ICC cell. This network starts to lose entrainment beyond a certain length which does not happen in an intact stomach. Gap junction studies in different biological systems suggest that Calcium ( $\text{Ca}^{2+}$ ) and Inositol trisphosphate ( $\text{IP}_3$ ) traverse between neighboring cells due to their concentration gradient. We implemented the idea in our model by adding  $\text{Ca}^{2+}$  and  $\text{IP}_3$  transport between neighboring ICC along with the existing electrical coupling. Now the first and last SM cell of the longer network have a constant phase delay in steady-state indicating entrainment and ICC and SM cells are in phase. The simulation results qualitatively match with the experimental recordings from the lower-mid corpus to the proximal antrum of the cat (Xue et al, 1995). The results suggest that, mere electrical coupling is not sufficient for creating entrainment along the entire length of the stomach.  $\text{Ca}^{2+}$  and  $\text{IP}_3$  transport may need to be considered while modeling an entire stomach.



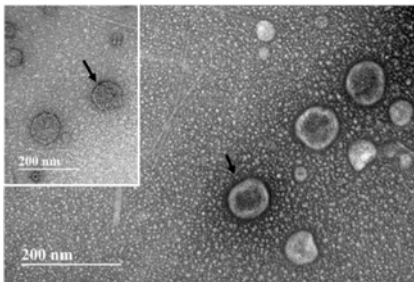
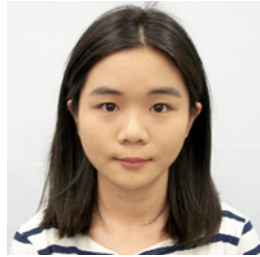
Representation of the proposed stomach model

# The Use of Optimized Stem Cell-Derived Exosomes in Facilitating Cardiac Regeneration

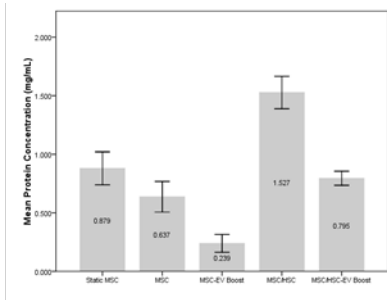
**Authors:** Yih-Mei Lin, Manuel Perez, Brittany Gonzalez, Reem Ekhraiwesh, Sharan Ramaswamy

**Faculty Advisor:** Sharan Ramaswamy, Ph.D.

Over the years, cardiovascular diseases (CVD) have become the major world-wide cause of mortality. Unfortunately, the heart has limited capability to regenerate from disease-inducing damage, which ultimately leads to heart failure eventually. Previous studies have shown that adult mesenchymal stem cells (MSCs) have the ability to differentiate into different cell types. However, MSCs have a low survival rate and suffer from suboptimal engraftment. An alternative approach in, cardiovascular regeneration may be via the delivery of the secretory factors released from MSCs. Exosomes are extracellular vesicles secreted by various cell types and thereby serve as a cargo of molecular factors which can deliver proteins, lipids and other constituents to a site of tissue damage and/or injury. In order to investigate the methods to enhance secretion of exosomes, our study involved a bioreactor device to create a mechanical flow environment to stimulate stem cells for this purpose. Moreover, we increased the MSC seeding density ( $\sim 35 \times 10^6$  cells) and incorporated a commercially-available biochemical exosome-augmenter (EV Boost™, Roosterbio, Frederick, MD) for additional elevated and rapid exosome production. Finally, CD 34+ hematopoietic stem cells (HSCs) ( $\sim 0.5 \times 10^6$  cells) were co-cultured with MSCs to explore the effect of HSCs on further increasing the quantity and quality of exosomal production via paracrine signaling. In this study, mass spectrometry, cytokines panel, and gene expression analysis techniques will be used to characterize the cardioprotective factors released from the exosomes. It is expected that these approaches will lead to an optimized bio-manufacturing protocol for producing stem cell-derived exosomes for more effective treatment of CVD than is currently available, via the induction of cardiac regenerative processes.



Transmission electron microscopy (TEM) of exosomes



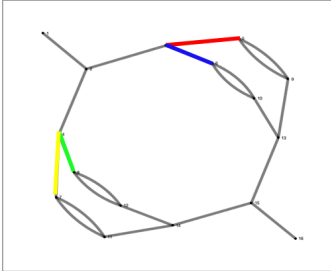
protein concentration

# Validation of Arterial Blood Stealing as a Mechanism of Negative BOLD Response

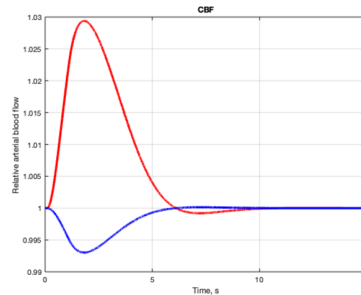
**Authors:** Alejandro Suarez, Jorge Riera Diaz

**Faculty Advisor:** Jorge Riera Diaz, Ph.D.

Blood Oxygen Level Dependent (BOLD) signal characterizes neuronal activity indirectly by measuring hemodynamic changes in the nearby microvasculature that are driven by neurovascular coupling phenomena (changes in arteriole diameter). Negative BOLD responses have been related to pathological neuronal activity, but also, they have been reported in regions surrounding normal neuronal activation (positive BOLD response). The origin of this negativity has generated a lot of discussion among researchers and many mechanisms have been proposed to explain this phenomenon. Blood flow “stealing” of one arteriole to another, both coming from the same bifurcation, could generate a negative BOLD response in the area fed by the arteriole with decreased flow. A model proposed to describe this mechanism consists in two windkessels connected by the same feeding artery including a solenoid to account for the inertial forces. In this work we validate the “stealing” effect through fluid dynamics simulations in a simple microvasculature using variable dilation amplitude in different arterioles and accounting for hematocrit changes. Furthermore, we performed parameter estimation to fit the results from the inductor-based model to the ones from the flow dynamics-based simulations in order to find the solenoid’s parameters that better describe the “stealing” phenomenon.

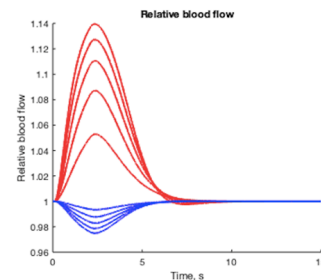
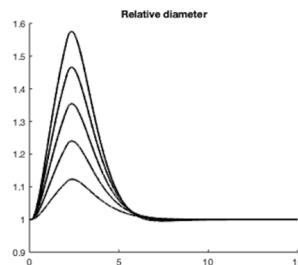


Microvascular network used to simulate blood flow dynamics



Blood flow “stealing” effect

Varying the amplitude of the stimulus.



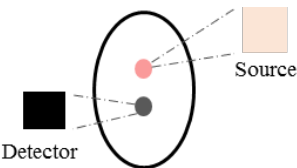


# Designing of Inclusive Wearables for Diverse Populations

**Authors:** Ajmal, Mel Tananant Boonya-ananta, Andres J. Rodriguez, Jessica C. Ramella-Roman

**Faculty Advisor:** Jessica C. Ramella-Roman, Ph.D.

Wearable devices are helping patients to monitor many chronic health conditions, such as diabetes and cardiovascular disease, outside the clinic. The ability of wearable to provide continuous monitoring makes them particularly suitable for the management of these chronic disorders which are disproportionately present in minorities. Compared to Caucasians, African American are 30% more likely to die of cardiovascular diseases, while Hispanic and Latino are 65% more likely to be diabetic. These groups have also significant higher rate of obesity. The motivation of our study, through Monte Carlo modeling, is to show how common optical wearable devices do not address the need of all users and are particularly limited in dealing with highly pigmented skin tones as well as large adipose layers. In this aspect, we performed the assessment of the hardware architecture of heart rate sensors in some of the commercially available wearables and modelled the PPG signal through Monte Carlo simulations. Through our studies, it is shown that the efficiency of these devices in monitoring HR is different in people with varying skin tone and BMI. Our aim is to come up with strategies to overcome these limitations and to develop optical wearable devices targeting chronic diseases.



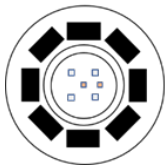
Nellcor: Clinical PPG system



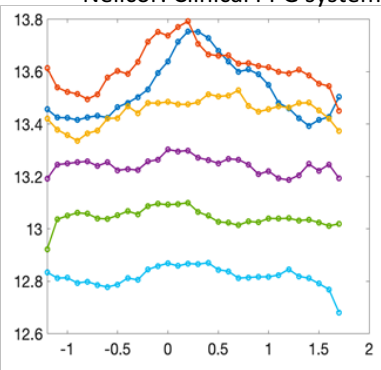
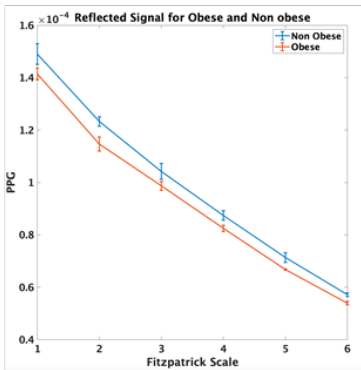
Apple iWatch



Fitbit Versa 2



Schematics of Heart rate sensors



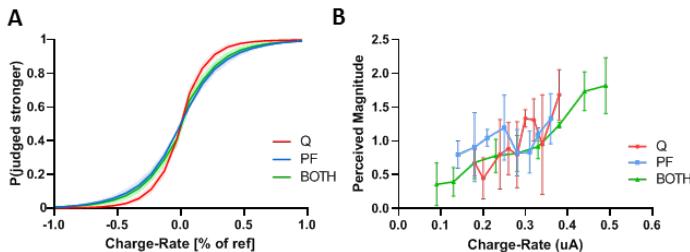
(Left): Photon counts reaching the detector, (Right); Simulated pulse shape for the PPG sensor, both in case of Apple iWatch S5.

# Charge-Rate Sensory Encoding with an Enhanced Surface Electrical Neurostimulation Platform

**Authors:** Andres Pena, Ranu Jung

**Faculty Advisor:** Ranu Jung, Ph.D.

Electrical stimulation of peripheral afferents has been used to study the sensory neural code and restore lost sensory function. Recently, deployment of implantable neural interfaces has prompted multiple breakthroughs in artificial somatosensory feedback for amputees, resulting in functional and psychological benefits. Although promising, the invasive nature of these approaches limits wide clinical applications, hindering the development of advanced neuromodulation strategies for intuitive sensory feedback. Transcutaneous stimulation is a potential non-invasive alternative to implantable systems. However, traditional methods are hampered by poor selectivity, skin discomfort, and limited percept modulation. An enhanced surface electrical neurostimulation platform has been developed to address the need for a non-invasive approach capable of selectively eliciting more comfortable distally-referred percepts than traditional methods. The ability to convey a wide range of discriminable levels of tactile intensities is critical to deliver task-related information such as grasping force. Tactile intensity is encoded in part by the total firing rate within the recruited afferent population. Simultaneous modulation of charge and frequency has been shown to influence fiber recruitment and rate with intraneural stimulation, enhancing percept intensity modulation. It was not known whether this charge-rate encoding strategy would also enhance intensity perception with surface stimulation. Classic psychophysical methods were used to probe the dependency of percept intensity on these parameters in able-bodied subjects with the surface stimulation platform, and in a transradial amputee with intrafascicular stimulation. In both cases, simultaneous charge and frequency modulation resulted in fine intensity discrimination and a wider dynamic range of intensities. These results provide compelling evidence that implementation of charge-rate encoding within the stimulation platform can address the percept modulation limitations of traditional methods. This may facilitate wide adoption of surface neurostimulation for chronic sensory restoration in amputees, and could serve as a non-invasive testbed for developing neuromodulation strategies before deployment in implanted systems.



Charge-rate determines perceived intensity

(A) Intensity discrimination: Able-bodied subjects reliably discriminated small increments of stimulation Q (15%), PF (23%), or both (20%).

(B) Magnitude estimation:

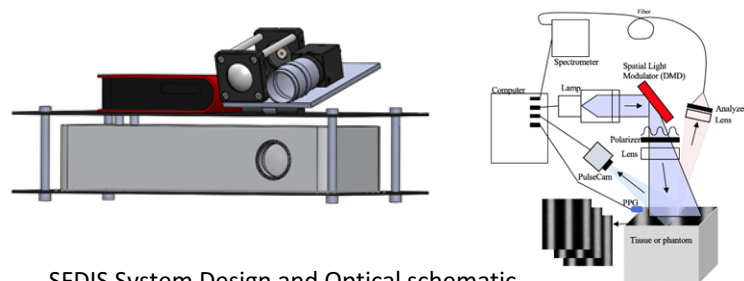
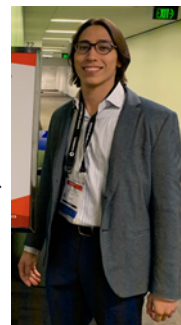
The amputee subject perceived a wider range of intensities with charge-rate modulation.

# Spatial Frequency Domain Imaging and Spectroscopic System for Quantifying Changes in Skin Optical Properties Effected by Alterations Related to Obesity

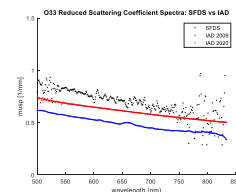
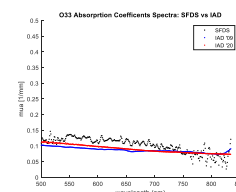
**Authors:** Andres J. Rodriguez, Mel Tananant Boonya-ananta, Vinh Nguyen Du Le, Jessica C. Ramella-Roman

**Faculty Advisor:** Jessica C. Ramella-Roman, Ph.D.

Obesity leads to a higher risk of diabetes and cardiovascular diseases. Wearable devices are used among the obese to manage and improve healthy lifestyles by measuring biomarkers; including heart rate, heart rate variability, perfusion, pressure pulse-wave velocities. To do so, wearables use optical sensors to capture fluctuations due to absorption of tissue. Individuals having a high Body Mass Index (BMI) with a thicker layer of adipose tissue scatter the signal, yielding poorer optical contrast and SNR. Moreover, higher BMI alters chemical concentrations—e.g., water, oxygenation, and blood volume in the dermal layer—and thus the optical properties (OP). Although OP of the skin exist in literature, no study has strictly recorded the effect and magnitude of a higher BMI on OP. We aim at constructing an imaging device to quantify the OP of the skin. We hypothesize individuals with higher BMI will show significant changes in OP. Our method of imaging will rely on an optical system combining Spatial Frequency Domain Imaging and Spectroscopy (SFDIS), which could be helpful in characterizing OP of the obese. SFDI separates and quantifies the absorption coefficient and reduced scattering coefficient by acquiring phase-shifted images and using the respective DC and AC components after demodulations, along with model calibrations, to solve and inverse problem, which yields 2-D maps of the OP of the sample imaged. Adding a spectrometer will aid in validating the resulting wavelength-specific OP. We will assemble, calibrate, and verify the workings of an SFDIS system on tissue-mimicking phantoms. The OP calculated should have insignificant error differences from phantoms' known properties. The system will be ready for in-clinic use to acquire the OP of larger cohorts. A larger study will aid in understanding how the anatomical and physiological changes in the obese skin affects the use optical sensors that record physiological biomarkers. Future works could help elucidating the world with better representative OP of the general ever-increasing obese population. Broadening light-tissue-interactions on the obese may aid the accuracy of wearable medical devices that monitor many of obesity's comorbidities.



SFDIS System Design and Optical schematic



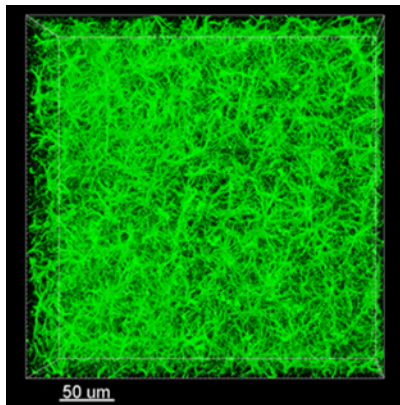
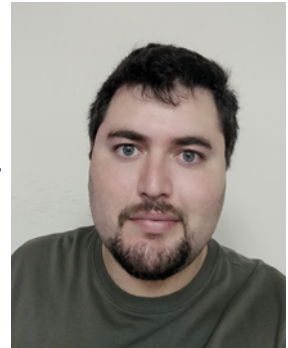
Calculated optical Properties of tissue-mimicking phantoms

# Analysis of the Murine Motor & Somatosensory Cortical Columns: Fractional Volume, Automated Nuclei Assignment and Astrocyte Morphological Analysis

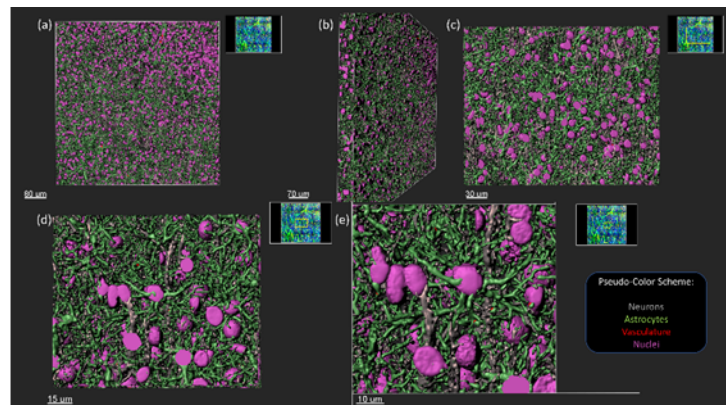
**Authors:** Jared Leichner, Wei-Chiang Lin

**Faculty Advisor:** Wei-Chiang Lin, Ph.D.

Within the dense cortical neuropil, analysis of morphology and density is complicated by a number of factors. First, interconnectivity of cellular components makes it extremely challenging to discern where individual cells begin and end. Second, intrinsic PSF-driven blurring during the imaging process anisotropically stretches imaged objects differently along the lateral and axial axes. In this work, we first develop an optimized staining and imaging scheme to collect neuronal, astrocytic, vascular and nuclear fluorescence simultaneously within entire cortical columns at high magnifications. Then, a wavelength and depth-dependent deconvolution scheme restores image quality by algorithmically reversing some of the PSF-driven blurring process during image formation. Afterwards, characterization of the fractional volume of each of the four imaging targets in a depth-dependent manner highlight the unique aspects of the motor and somatosensory functional regions. Finally, an automated nuclei identification algorithm identifies astrocytic nuclei using the four-channel fluorescence data and allows for unique astrocyte identification and subsequent morphological analysis. This collection of protocols aims to enhance existing immunofluorescent staining and imaging procedures, provide valuable metrics of fractional volume of these components in unique functional regions, demonstrate the potential for automated astrocyte identification and uncover patterns of morphological heterogeneity of astrocytes in a region-specific and cortical depth-dependent manner.



Astrocyte Density in the Neuropil



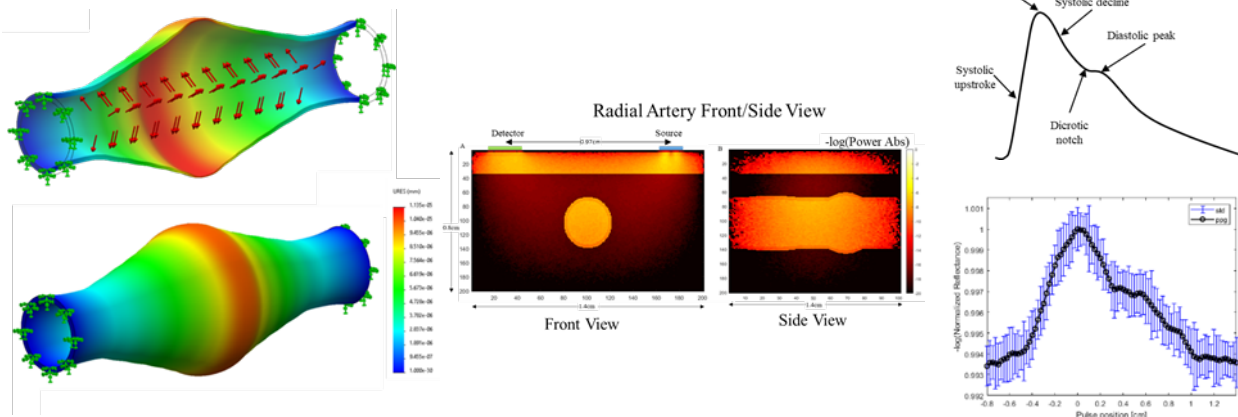
Volumetric Modeling & Sequential Zooming of Four-Channel Data

# Modeling of a Photoplethysmographic (PPG) Waveform through Monte Carlo as a Method of Deriving Blood Pressure in Individuals with Obesity

**Authors:** Mel Tananant Boonya-ananta, Andres J. Rodriguez, Anders K. Hansen, Joshua D. Hutcheson, Jessica C. Ramella-Roman

**Faculty Advisor:** Jessica C. Ramella-Roman, Ph.D.

Systolic and diastolic blood pressure values can be used as an indicator of an individual's risk for cardiovascular disease. The common practice of blood pressure (BP) measurement using a cuff-based system provides a snapshot of blood pressure at a single instance in time and can be inconvenient and intrusive. The development of optical methods to determine blood pressure could provide continuous monitoring of blood pressure through techniques such as pulse transit time (PTT) or pulse arrival time (PAT) when used with echocardiogram. Cuff based BP devices are known to have variation and inaccuracies when applied to larger arm sizes as seen in individuals with obesity but little is known of the influence of obesity in the PPG/PTT and PAT signals. We propose that accurate waveform replication is required for the derivation of blood pressure applied to individuals with obesity. Here we use the Monte Carlo framework to develop the PPG waveform as a means to derive blood pressure through cuff less techniques. The development of a simulated waveform incorporates realistic changes in the artery related to its biomechanical properties as a pressure wave is propagated through the vessel. It is shown that a change in vessel pressure and geometry directly affects the captured optical signal. The system can account for variations in body-mass index to compensate for geometrical changes in adipose tissue layer and changes in optical properties.



(Left): Simulated arterial dilation  
(Middle): Monte Carlo geometry view of pulse propagation  
(Right): Generated PPG Waveform

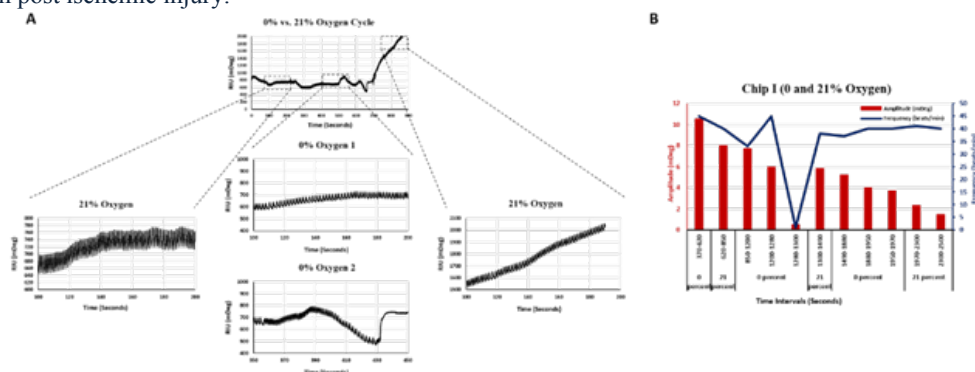


# Plasmonic Tracking of Cardiac Cells' Functional Behavior in Response to Ischemic Injury

**Authors:** Maedeh Mozneb, Chen-Zhong Li

**Faculty Advisor:** Chen-Zhong Li, Ph.D.

In understanding in vitro cardiac systems for disease modeling, drug testing and development of effective heart-on-chip devices, a well-established knowledge of cardiac tissue's functionality, respiration and metabolism is highly essential. As a portion of tissue metabolism, effect of oxygen concentration on cardiac cell function is known to be highly vital for development of a synchronized and strong contraction profile. However, monitoring the effect of oxygen on cellular behavior, especially in a tissue format, requires extensive labeling of cells or complicated microfabricated devices. Here we are presenting a follow up of our previous study. Surface Plasmon Resonance (SPR) is used as a label-free optical technique to track contraction profile of cardiac cells in response to different oxygen content media. Cardiomyocytes' cultured gold chips are exposed to 0%, 5% and 10% oxygen content media to simulate a perfused ischemic injury on the cells. The media is then switched to oxygen rich controls (21%) and cell contraction recovery is evaluated post ischemic injury based on signal frequency and amplitude. Our observations indicate that SPR is highly fast and sensitive in detecting functional changes of cardiac cells based on their environmental oxygen content change. We have also observed based on our two experimental samples (n=2) that 10% oxygen content media provides the most efficient amount of oxygen for recovering purposes of cardiac cell contraction post ischemic injury.



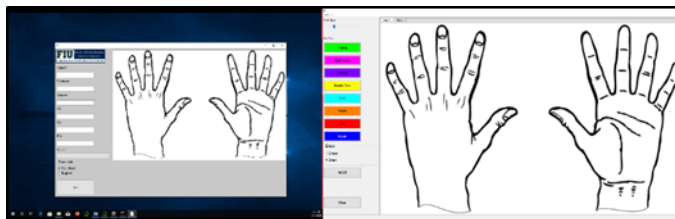
A) SPR signal of different oxygen content media injections on cardiac cells. From left to right: initial injection of 21% oxygen content media, two different intervals post injection of 0% oxygen media and re-injection of 21% oxygen media. Cell's beating profile is steady at first, followed by a decrease in beat and potency, which resulted in a fast beating which is then stopped. The beating is reinstated as the cells are slowly getting introduced to 21% oxygen content media. B) graph shows amplitude of beating signal (potency of beat) and frequency of beats over multiple cycles of media switch. (n=2).

# Analysis and Development of a Digital Survey Tool for Recording Perceived Sensory Feedback on Peripheral Nerve Stimulation

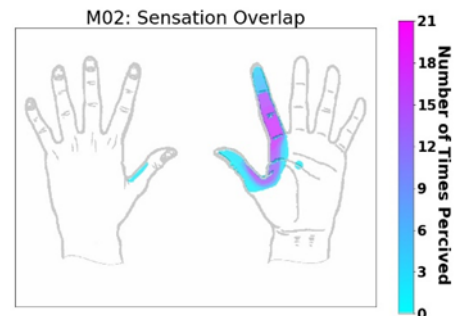
**Authors:** Tommaso Benigni Sathyakumar Kuntaegowdanahalli, Andres Pena, Anil Thota, James Abbas, Ranu Jung

**Faculty Advisor:** Ranu Jung, Ph.D.

In an on-going clinical trial of a Neural-Enabled Prosthetic Hand system in individuals with upper-limb amputation, sensory percepts elicited on electrical stimulation of nerve fibers in peripheral nerves of the residual limb are being characterized. Currently, the individual reports the location and type of sensation perceived on the phantom hand by coloring a picture of a blank hand drawing in a sensation survey form. The process is repeated over multiple study sessions conducted over multiple months. Each form has to be digitized before useful quantitative information such as total perceived area and centroid of the area can be extracted. The digitized versions are stacked to assess stability of the percept location over time. To address the shortcomings of the current process a digital tablet based software tool was created. Requirements such as data accuracy, data safety, ease of use and accessibility were identified. The tool includes a GUI interface where subjects can draw perceived sensations on a digital image of a hand. In order not to interfere with subjects during this drawing process, a secondary experimenter window where annotation and supervision of the data can take place was created as well. In order to maintain data safety, once the drawing is complete the survey is saved as a raw copy, processed into an analyzable copy and stored in an excel based data structure. In order to address accessibility, oversized buttons and other widgets were added. Analysis tools to quantify percept area and centroids of multiple overlays will also be implemented. The tool can also be expanded for use in other experimental studies that require subject feedback to characterize their perceived sensations by simply changing the background image of the GUI.



Sensation Survey Tool Front End



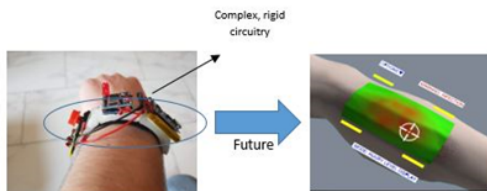
Overlay of perceived sensations over multiple study sessions. The same electrode (M02) was stimulated in each session.

# 3D Heterogeneous and Flexible Package Integration for Zero-Power Wireless Neural Recording

**Authors:** Sk Yeahia Been Sayeed, P. Markondeya Raj, John Volakis

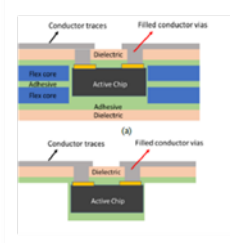
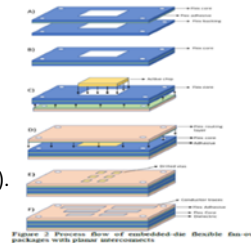
**Faculty Advisors:** P. Markondeya Raj, Ph.D.; John Volakis, Ph.D.

Personal medical care requires accurate, reliable, robust, low power and low-cost methods to sense changes in biophysical signals and communicate them to a device or a base station for autonomous health monitoring. The conventional neural signal recording system uses batteries that power up the wireless neural recording systems or sensors. Most importantly, when wearable and implantable devices use power from the onboard battery, it causes the temperature to rise beyond the safety level. Moreover, for implantable neural recording, elevated temperature can affect the human tissue significantly, while changing or replacing physical battery requires invasive surgery. Having a battery or batteries for on-skin sensing patches is highly likely harmful for the human body and have very limited lifespan. A zero-power wireless neural recording sensor, in other words, having no power-consuming active components in the system, which uses radio-frequency input and radio-frequency output by dual antennas and passive multiplier and mixer, is highly desirable the key building block advances towards this 3D integration of thinned dies in packages with fanout interconnects. Miniaturized antennas are designed with high-permittivity flexible substrates with permittivity of  $\sim 10$  and loss tangent of 0.002. Moreover, passive mixer and multiplier chips are embedded in a flex substrate and silver elastomer composite paste is used to form the via contacts to the die pad and realize reliable interconnects that are resilient to mechanical deformation and strain, antennas and chips. The flex substrate acts as the dielectric surface for supporting the printed conductor traces.

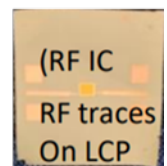
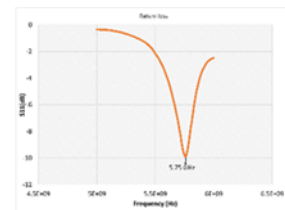


Traditional Bulky and active component-based sensor (courtesy by <https://www.rs-online.com/designspark/wearable-fall-detector> (left); Proposed prototype miniaturized zero power wireless neural(right).

Process flow of embedded-die flexible fan-out packages with planar interconnects(left).



Package-integrated antennas for wireless sensing (left and middle), High density flex circuitry (right).



# Correlating Aortic Valve Structure to Heart Sound Characteristics

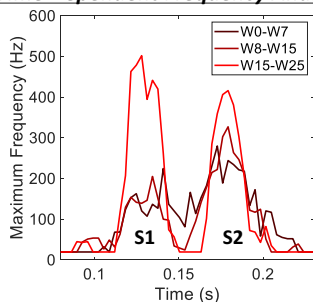
**Authors:** Valentina Dargam, Amiral Bakshian Nik, Joshua Hutcheson

**Faculty Advisor:** Joshua Hutcheson, Ph.D.

Aortic valve disease (AVD) occurs when aortic valve leaflets become thickened and stiff due to fibrotic remodeling and formation of calcific nodules. AVD is the most common valve disease and patients may experience no symptoms until the disease has progressed significantly. Asymptomatic patients are not referred to specialists for advanced imaging procedures that can diagnose AVD. Better screening strategies that can be implemented into routine physical examinations are needed to detect AVD, regardless of symptom manifestation. The vibrations of aortic valve leaflets during valve closure produce the audible frequencies heard through a doctor's stethoscope. In this study, we hypothesize that microstructural alterations during aortic valve remodeling cause changes in the valvular acoustic characteristics prior to gross changes in valve performance. Starting at 10-weeks of age, 8 ApoE-KO mice were fed an atherogenic diet and heart sounds were recorded weekly. At 35-weeks of age, the mice were sacrificed for analysis of mineral growth. Preliminary results show changes over the course of the experiment in both the time and frequency domains. The dominant frequency of the S2 sound increases as early as 15 weeks, at early stages of valve remodeling prior to changes in valve performance. Principle component analysis (PCA) shows that the first principle component segregates heart sounds associated with time points prior to valve remodeling, early remodeling with preserved valve function, and late stages with altered valve function. The outcomes of the proposed research can contribute to the future development of a non-invasive diagnostic tool to identify patients with different stages of AVD.

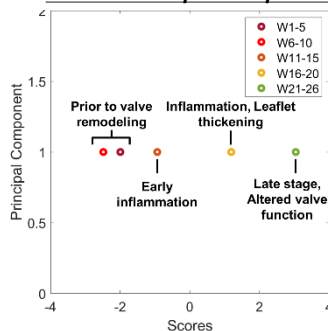


## Time Dependent Frequency Analysis



Time and frequency characteristics of heart sounds of one mouse over the course of 25-weeks show an increase in the dominant frequencies of the each sound (S1 and S2).

## PCA Variance per Component



PCA analysis shows changes in the first principal component in relation to aortic valve remodeling (n=8).

## ABOUT OUR PROGRAM

*The Department of Biomedical Engineering (BME) is part of the College of Engineering and Computing at FIU and is a prime resource for biomedical engineering education, training, research, and technology development. BME is an ever-evolving field that uses and applies engineering principles to the study of biology and medicine in order to improve health care.*

*Located in Miami, Florida, Florida International University, a Top 100 public university that is designated a Carnegie Highest Research (R1) and Carnegie Community Engaged institution is committed to high-quality teaching, state-of-the-art research and creative activity, and collaborative engagement with the local and global communities.*

*The Graduate Program of the Department of Biomedical Engineering is ranked in different categories, providing the best value to students nationally: #12 best BME master (College Choice), # 26 most popular (College Factual), #43 (Best Value Schools), and #43 best public (Grad Schools, USNews). We are preparing a diverse community of biomedical engineers and are engaged in translation of research to health care applications through discovery, innovation, entrepreneurship, and community engagement.*

***bme.fiu.edu***  
***@fiubiomed***  
***(305) 348-6950***





***Be Worlds  
Ahead***

*DISCOVER DESIGN DEVELOP DELIVER*



**FIU** | Engineering  
& Computing  
Biomedical Engineering